Brief Research Report | Intervention

eISSN 2005-8330
https://doi.org/10.3348/kjr.2022.0140
Korean J Radiol 2022;23(8):794-802

Korean Journal of Radiology
KJR

Feasibility of Single-Shot Whole Thoracic Time-Resolved MR Angiography to Evaluate Patients with Multiple Pulmonary Arteriovenous Malformations

Jihoon Hong[1], Sang Yub Lee[1], Jae-Kwang Lim[1], Jongmin Lee[1], Jongmin Park[1], Jung Guen Cha[1], Hui Joong Lee[1], Donghyeon Kim[2]

[1]Department of Radiology, School of Medicine, Kyungpook National University, Kyungpook National University Hospital, Daegu, Korea; [2]Department of Radiology, Gyeongbuk Regional Rehabilitation Hospital, Gyeongsan, Korea

Objective: To evaluate the feasibility of single-shot whole thoracic time-resolved MR angiography (TR-MRA) to identify the feeding arteries of pulmonary arteriovenous malformations (PAVMs) and reperfusion of the lesion after embolization in patients with multiple PAVMs.

Materials and Methods: Nine patients (8 females and 1 male; age range, 23–65 years) with a total of 62 PAVMs who underwent percutaneous embolization for multiple PAVMs and were subsequently followed up using TR-MRA and CT obtained within 6 months from each other were retrospectively reviewed. All imaging analyses were performed by two independent readers blinded to clinical information. The visibility of the feeding arteries on maximum intensity projection (MIP) reconstruction and multiplanar reconstruction (MPR) TR-MRA images was evaluated by comparing them to CT as a reference. The accuracy of TR-MRA for diagnosing reperfusion of the PAVM after embolization was assessed in a subgroup with angiographic confirmation. The reliability between the readers in interpreting the TR-MRA results was analyzed using kappa (κ) statistics.

Results: Feeding arteries were visible on the original MIP images of TR-MRA in 82.3% (51/62) and 85.5% (53/62) of readers 1 and 2, respectively. Using the MPR, the rates increased to 93.5% (58/62) and 95.2% (59/62), respectively (κ = 0.760 and 0.792, respectively). Factors for invisibility were the course of feeding arteries in the anteroposterior plane, proximity to large enhancing vessels, adjacency to the chest wall, pulsation of the heart, and small feeding arteries. Thirty-seven PAVMs in five patients had angiographic confirmation of reperfusion status after embolization (32 occlusions and 5 reperfusions). TR-MRA showed 100% (5/5) sensitivity and 100% (32/32, including three cases in which the feeding arteries were not visible on TR-MRA) specificity for both readers.

Conclusion: Single-shot whole thoracic TR-MRA with MPR showed good visibility of the feeding arteries of PAVMs and high accuracy in diagnosing reperfusion after embolization. Single-shot whole thoracic TR-MRA may be a feasible method for the follow-up of patients with multiple PAVMs.

Keywords: *Time-resolved MR angiography; Pulmonary arteriovenous malformation; Computed tomography; Transcatheter embolization; Reperfusion*

INTRODUCTION

Pulmonary arteriovenous malformations (PAVMs) have a right-to-left shunt that can cause life-threatening complications such as stroke or brain abscesses [1]. Transcatheter embolization is the treatment of choice for PAVM, and a high technical success rate has been reported [2-5]. However, even after successful embolization, PAVM patency due to recanalization or reperfusion is emerging as an important issue [6-8] because it can cause neurologic

Received: March 4, 2022 **Revised:** March 27, 2022 **Accepted:** June 6, 2022
Corresponding author: Sang Yub Lee, MD, Department of Radiology, School of Medicine, Kyungpook National University, Kyungpook National University Hospital, 680 Gukchaebosang-ro, Jung-gu, Daegu 41944, Korea.
• E-mail: lsyrad@gmail.com

Korean Journal of Radiology
KJR

complications [9]. Therefore, an accurate, noninvasive, and easily accessible follow-up modality is required to monitor treatment failure. CT is used as the standard follow-up modality [9,10]; however, the widely used 70% criteria for venous sac or draining vein reduction have low specificity issues [11-13].

In recent years, time-resolved MR angiography (TR-MRA) has shown potential as a novel follow-up modality after PAVM treatment [14-16]. This technique demonstrates the flow dynamics of a PAVM without radiation exposure. However, previous TR-MRA studies mainly focused on one PAVM per single contrast injection [17]. Their studies showed limited efficacy in applying this modality to multiple PAVMs due to limited acquisition volume or failure to match CT [14,17]. However, the authors postulated that if single-shot whole thoracic TR-MRA was performed based on a 3T MR system with a high signal-to-noise ratio (SNR), TR-MRA could be used for multiple PAVMs when each lesion was matched 1-to-1 with CT. Therefore, this study aimed to investigate whether single-shot whole thoracic TR-MRA could be used to identify the feeding arteries of the PAVM and reperfusion of the lesion after embolization in patients with multiple PAVMs.

MATERIALS AND METHODS

Study Design and Patient Selection

This retrospective study was approved by the Institutional Review Board of the Kyungpook National University Hospital (IRB No. 2019-12-026). Patients who underwent percutaneous embolization for PAVM between August 2008 and March 2021 were reviewed. To evaluate the efficacy of TR-MRA in the follow-up of multiple PAVMs, eligible patients were identified using the following inclusion criteria: 1) patients with multiple (≥ 2) PAVMs, 2) patients treated with percutaneous embolization therapy using coils or vascular plug, and 3) post-embolization imaging follow-up with CT and TR-MRA performed within 6 months of each other. A total of nine patients (8 females and 1 male; mean age, 47.3 years; age range, 23–65 years) with 62 PAVMs met the criteria (Fig. 1). Electronic medical records were reviewed for data analysis to evaluate clinical history, physical examination, and characteristics of PAVM.

CT and Single-Shot Whole Thoracic TR-MRA Techniques

Initial and follow-up CT before and after endovascular embolization was performed mainly using contrast-enhanced

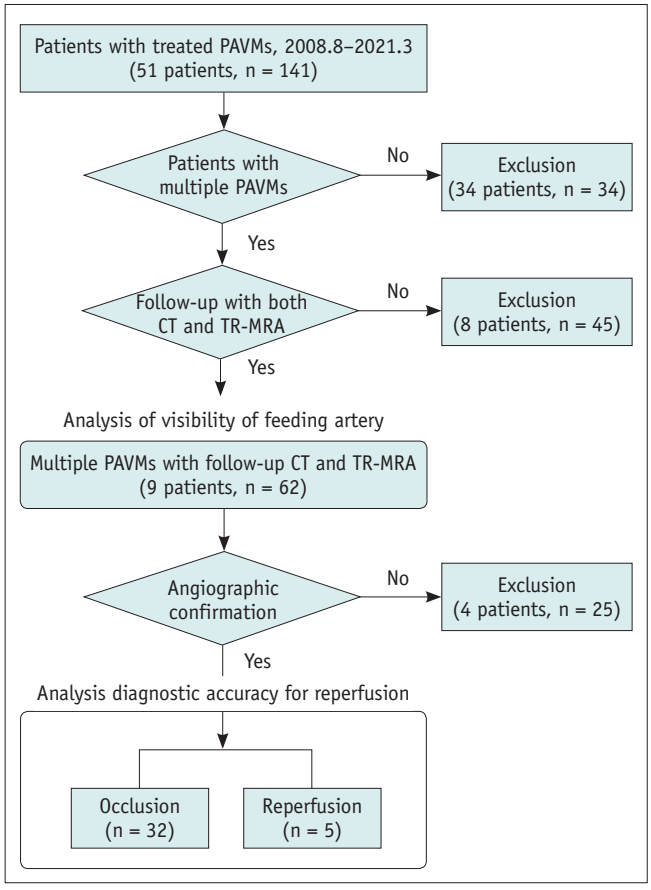

Fig. 1. Flow chart summarizing patient enrollment according to study eligibility criteria. n = indicates the number of PAVMs, PAVM = pulmonary arteriovenous malformation, TR-MRA = time-resolved MR angiography

CT with multidetector-row scanners. For the examination, 80–100 mL of contrast medium was injected intravenously at a rate of 1.5–2 mL/s. CT images of the area of interest were reconstructed with a 2.5-mm slice thickness in transverse coronal orientation. Follow-up CT was performed at approximately 6 and 12 months and every 2–3 years after PAVM embolization.

All TR-MRAs were performed using a 3T MR system (Signa Architect; GE Healthcare) with a 16-channel cardiac coil. Each acquisition slab was set to maximally cover the entire lung, and images were taken based on a three-dimensional (3D) T1-weighted gradient echo sequence after injection of 0.15 mmol/kg of gadolinium-based contrast (ProHance; Bracco Imaging) at a flow rate of 2 mL/s and saline flushing after breath-hold. The acquisition parameters were as follows: repetition time, 4 ms; echo time, 1 ms; flip angle, 40°; field of view (FOV), 370 mm; matrix, 320 x 192; slice thickness, 5 mm interpolated to 2.5 mm. We acquired 56–71 slices to cover the thickness of the slab, which

 https://doi.org/10.3348/kjr.2022.0140

included the entire lung. Consequently, a voxel size of 1.2 x 1.9 x 2.5 mm^3 and temporal resolutions between 1.6 and 1.8 seconds were achieved, and 25 frames of 3D volume were acquired successively. Each frame was reconstructed using a maximum intensity projection (MIP) algorithm.

Image Analysis and Interpretation

All imaging analyses were performed by two independent and experienced cardiovascular radiologists. They were not involved in the clinical diagnosis of PAVMs or follow-up imaging. The outcomes of PAVM embolization, including data and clinical information, were not provided for blinded

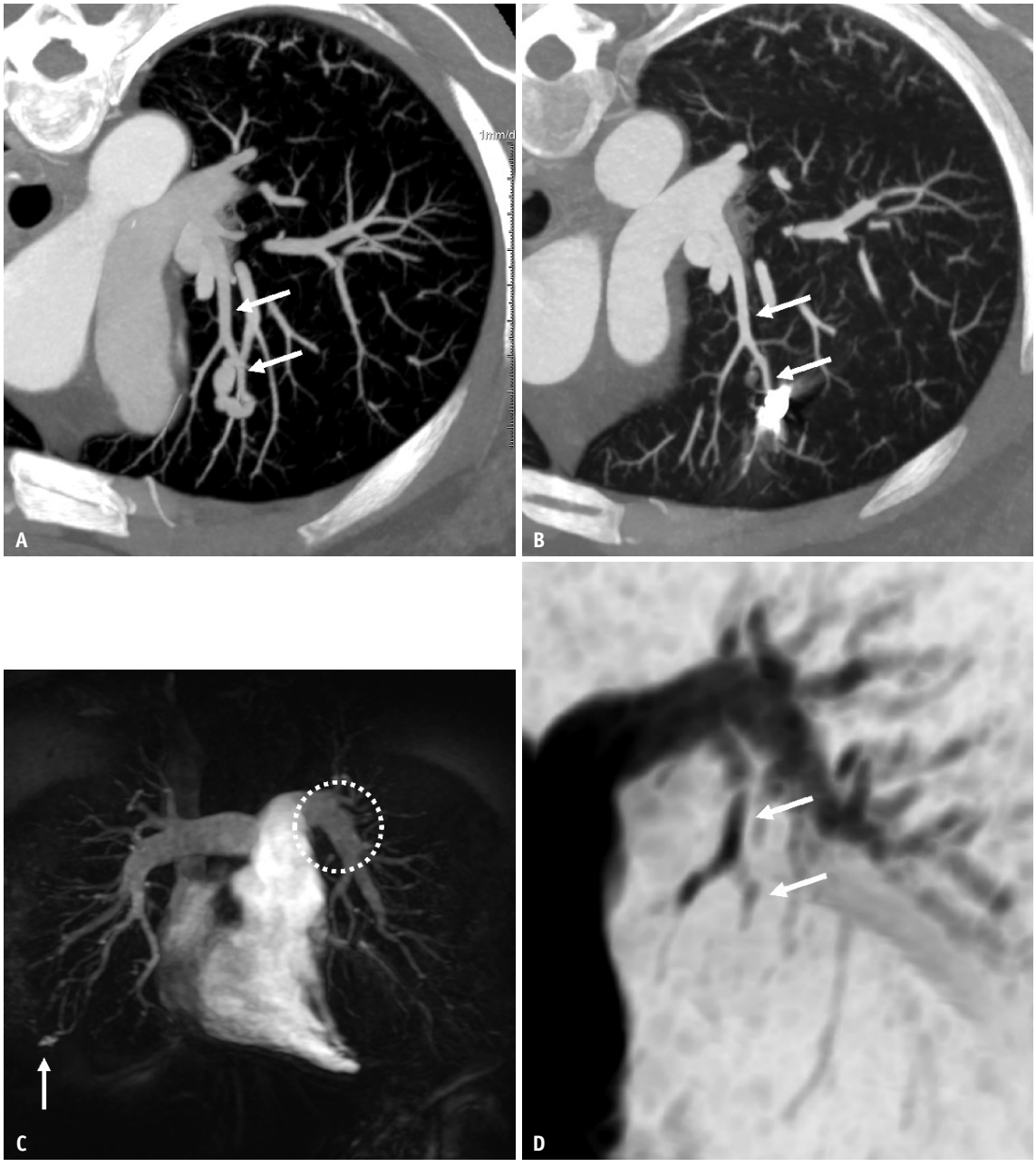

Fig. 2. A 40-year-old female patient underwent coil and vascular plug embolization for three out of four PAVMs located in the left lingular division of the upper lobe and lower lobe.
A. The MIP CT image shows the anteroposterior location of the PAVM. Feeding arteries are noted (arrows). **B.** Multiplanar reconstructed CT image of 6 months of follow-up. Feeding arteries are noted (arrows). **C.** The original MIP-reconstructed TR-MRA demonstrates that the anteroposteriorly located PAVM is obscured by the left inter-lobar pulmonary artery (dashed circle). **D.** After separating the overlapped structure by adjusting the angle through the multiplanar reconstruction of TR-MRA, the matched feeding artery (arrows) is clearly depicted on CT **(B)**. One untreated small PAVM is clearly identified in the whole thoracic TR-MRA (arrow in **C**). MIP = maximum intensity projection, PAVM = pulmonary arteriovenous malformation, TR-MRA = time-resolved MR angiography

https://doi.org/10.3348/kjr.2022.0140

Korean Journal of Radiology
KJR

analysis.

The location, complexity (simple vs. complex), and changes in vessel diameter on preprocedural and postprocedural CT (including feeding artery, venous sac, and draining vein) of PAVMs were reviewed. A simple PAVM is characterized by one or more afferent feeding arteries that originate from a single segmental pulmonary artery, while a complex PAVM is defined as multiple afferent feeding arteries that originate from several segmental arteries [18]. The embolic materials used for embolization and the embolization level (feeding artery embolization vs. venous sac embolization) were also reviewed.

Table 1. Characteristics of Patients, PAVMs, Embolization Procedures, and Follow-Up

Parameters	Value
Patient parameter (n = 9)	
Male, female	1 (11.1), 8 (88.9)
Mean age (range), year	47.3 (23–65)
Symptomatic	5 (55.6)
Number of PAVMs per patient	
2–5	5
> 5	4
PAVM parameter (n = 62)	
RUL, RML, RLL	9 (14.5), 15 (24.2), 12 (19.3)
LUL, LLL	10 (16.1), 16 (25.8)
Simple, complex	60 (96.8), 2 (3.2)
Mean preprocedure FAD (range), mm	3.01 (1.50–4.90)
Mean postprocedure FAD (range), mm	2.01 (0.89–4.16)
Postprocedure FAD categories, mm	
< 1.5	5
≥ 1.5, < 2	36
≥ 2, < 3	16
≥ 3	5
Embolization parameter (n = 62)	
FAE, VSE	46 (74.2),16 (25.8)
Coils, AVP, AVP + coils	26 (41.9), 35 (56.5), 1 (1.6)
Follow-up	
Mean time from embolization to TR-MRA (range), day	637.5 (4–1567)
Mean time between CT and TR-MRA (range), day	98 (1–182)

Data are number of patients or PAVMs with percentage in parentheses, unless specified otherwise. AVP = Amplatzer vascular plug, FAD = feeding artery diameter, FAE = feeding artery embolization, LLL = left lower lobe, LUL = left upper lobe, PAVM = pulmonary arteriovenous malformation, RLL = right lower lobe, RML = right middle lobe, RUL = right upper lobe, TR-MRA = time-resolved MR angiography, VSE = venous sac embolization

The visibility of the feeding arteries proximal to embolic materials on single-shot whole thoracic TR-MRA was evaluated for all PAVMs by correlating TR-MRA with CT images as a reference. All feeding arteries were identified by comparing preprocedural and postprocedural CT images. The feeding arteries were then examined using TR-MRA images. The search was first performed using coronal whole thoracic MIP TR-MRA imaging, which was subtracted and automatically reconstructed, and subsequently using multiplanar reconstruction (MPR) TR-MRA imaging on a 3D workstation (AW server 3.2; GE Healthcare) (Fig. 2). If the feeding artery proximal to the embolic material could be found in TR-MRA, the reader recorded a positive match. If the feeding arteries were not visible on TR-MRA, the reasons for invisibility were analyzed and reported in consensus between the two readers.

The diagnostic accuracy of TR-MRA in the identification of reperfusion after embolization was evaluated in angiographically confirmed cases. During multiple PAVM treatments with multiple sessions, previously treated lesions were checked by angiography. Segmental or selective pulmonary angiographic images of previously treated lesions were used for angiographically confirmed case analysis. Reperfusion of PAVM in TR-MRA was defined as the simultaneous enhancement or visualization of a venous sac and draining vein in the pulmonary arterial phase [14-16].

Inter-reader reliability was assessed using kappa (κ) statistics. Medcalc version 19.4.1 (Medcalc software Ltd.) was used for the analysis.

Table 2. Visibility of Feeding Arteries on TR-MRA Compared with CT as the Reference

	Original MIP TR-MRA (%)		MPR TR-MRA (%)	
	Matching + (i.e., Visible)	Matching -	Matching + (i.e., Visible)	Matching -
Reader 1	51 (82.3)	11 (17.7)	58 (93.5)	4 (6.5)
Reader 2	53 (85.5)	9 (14.5)	59 (95.2)	3 (4.8)
Average	52 (83.9)	10 (16.1)	58.5 (94.4)	3.5 (5.6)

Matching + and - as compared with CT indicate visibility and invisibility, respectively, of feeding arteries on TR-MRA. MIP = maximum intensity projection, MPR = multiplanar reconstruction, TR-MRA = time-resolved MR angiography

https://doi.org/10.3348/kjr.2022.0140

RESULTS

A total of 62 PAVMs in nine patients (2–20 lesions per patient) were analyzed. The characteristics of the patients, PAVMs, embolization procedures, and follow-up are summarized in Table 1.

The visibility of the feeding arteries in TR-MRA assessed by matching TR-MRA with follow-up CT as reference is summarized in Table 2. In comparison, the matching positive (i.e., visibility of feeding arteries on TR-MRA) rates between the original MIP-reconstructed TR-MRA and CT were 51/62 (82.3%) and 53/62 (85.5%) for reader 1 and reader 2, respectively. When each reader analyzed the MPR TR-MRA images on a 3D workstation, the matching positivity increased to 58/62 (93.5%) and 59/62 (95.2%), respectively. The κ between the two readers were 0.760 and 0.792 for the original MIP and MPR images, respectively.

The factors for the invisibility of feeding arteries in TR-MRA are summarized in Table 3, and examples are shown in Figures 3 and 4.

Regarding the diagnostic accuracy of identifying reperfusion of PAVMs after embolization, 37 PAVMs in five patients were confirmed angiographically during multiple treatment sessions (32 occlusions and 5 reperfusion). Both readers demonstrated 100% (5/5) sensitivity and 100% (32/32, including three cases in which the feeding arteries were not visible on TR-MRA) specificity on TR-MRA to diagnose reperfusion of PAVMs (κ, 1).

Table 3. Factors for Invisibility of Feeding Arteries on TR-MRA

	Original MIP TR-MRA		MPR TR-MRA	
	Reader 1 (n = 62)	Reader 2 (n = 62)	Reader 1 (n = 62)	Reader 2 (n = 62)
Feeding artery course on anteroposterior plane	7 (11.3)	6 (9.7)	-	-
Obscured by normal enhancing large vessels (BCV, SVC, right heart, and other PAs)	6 (9.7)	6 (9.7)	-	-
Location adjacent to chest wall	1 (1.6)	1 (1.6)	-	-
Pulsation of heart	1 (1.6)	1 (1.6)	1 (1.6)	1 (1.6)
Small diameter feeding artery	3 (4.8)	2 (3.2)	3 (4.8)	2 (3.2)
Total	11 (17.7)	9 (14.5)	4 (6.6)	3 (4.8)

Data are number of pulmonary arteriovenous malformations with the percentage in parentheses. BCV = brachiocephalic vein, MIP = maximum intensity projection, MPR = multiplanar reconstruction, PA = pulmonary artery, SVC = superior vena cava, TR-MRA = time-resolved MR angiography

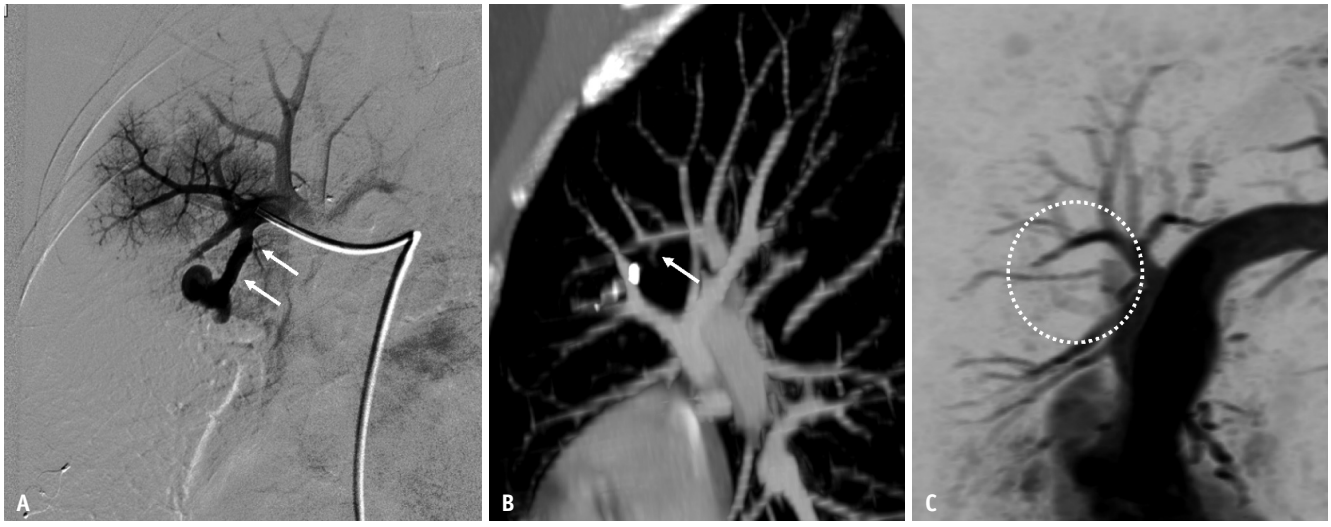

Fig. 3. A 49-year-old female patient underwent coil and vascular plug embolization for bilateral 12 pulmonary arteriovenous malformations. Eleven out of 12 feeding arteries on CT were identified using the original TR-MRA (n = 10) and additionally in multiplanar reconstruction (n = 1).
A. Selective angiography at the time of the procedure shows the feeding artery (arrows) and the segmental artery from which it arises. **B.** The follow-up CT with maximum intensity projection revealed a markedly decreased diameter of the feeding artery (1.31 mm) (arrow) that is difficult to measure even with CT. **C.** The multiplanar reconstructed TR-MRA failed to visualize the small feeding artery closest to the embolic material due to limited spatial resolution (dashed circle). TR-MRA = time-resolved MR angiography

https://doi.org/10.3348/kjr.2022.0140

Korean Journal of Radiology
KJR

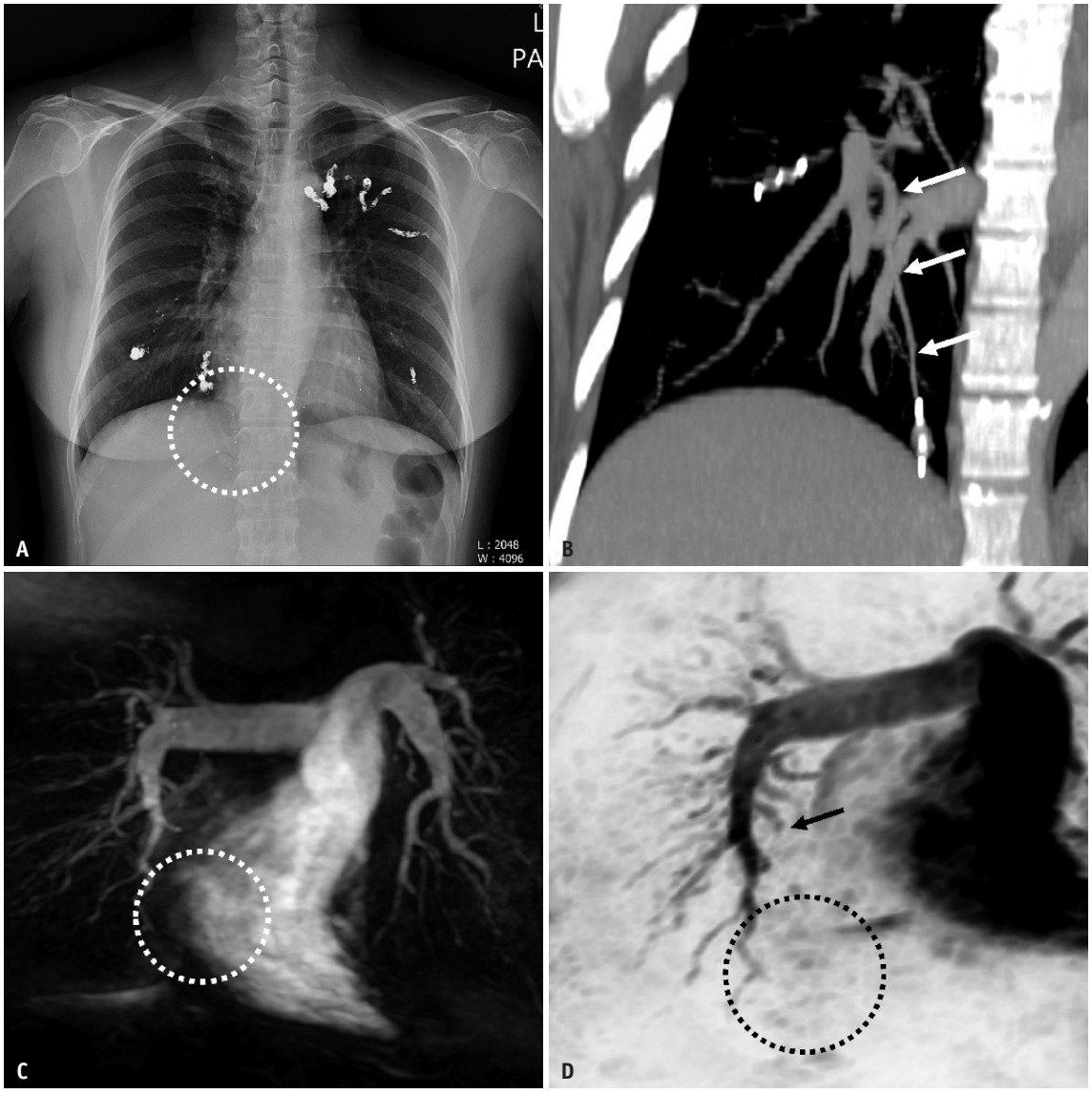

Fig. 4. A 44-year-old female patient underwent coil and vascular plug embolization for bilateral 20 PAVMs. Of the 20 PAVMs, 19 feeding arteries were shown in TR-MRA, matching the findings in CT (in original TR-MRA in 14 and in reconstructed TR-MRA in an additional 5). **A.** The chest X-ray showed multiple embolic materials in the bilateral lung fields, including the pericardiac location (dashed circle). **B.** Maximum intensity projection CT image shows a small feeding artery (arrows). **C, D.** The matching of the feeding artery (arrow) between CT and TR-MRA failed in both the original **(C)** and multiplanar reconstruction **(D)** TR-MRA. The cause of the blurred image was postulated as a heartbeat-induced motion artifact (dashed circles in **C** and **D**). PAVM = pulmonary arteriovenous malformation, TR-MRA = time-resolved MR angiography

DISCUSSION

To evaluate the outcomes of PAVM embolization in TR-MRA, finding each feeding artery compared to preprocedural CT is essential. In the present study, single-shot TR-MRA for multiple PAVMs showed good visibility of the feeding arteries compared to CT, which further improved with the use of the MPR technique. The diagnostic accuracy of TR-MRA for reperfusion after PAVM embolization was high.

TR-MRA has demonstrated high diagnostic accuracy (sensitivity and specificity > 90%) as a follow-up modality after PAVM embolization [14]. This modality has several benefits compared with static CT imaging, such as being radiation-free and providing flow information [14,17]. The hemodynamic characteristics of untreated or reperfused PAVMs in TR-MRA include early venous return through the fistula, which simultaneously visualizes the pulmonary vein in the pulmonary arterial phase. Metallic artifacts from embolic materials (especially metallic coils over vascular plugs) obscure changes in draining vein diameter

 https://doi.org/10.3348/kjr.2022.0140

during CT evaluation. In particular, tightly packed coil nests create a large area of metallic artifacts on CT [4,14]. Minimal blurring artifacts can also be seen on TR-MRA; however, regarding metallic artifacts, TR-MRA showed better resolution for detecting non-shrinkage pulmonary veins or venous sacs, especially in small-sized vessels, due to high SNRs on CT images.

However, there is limited evidence regarding the application of TR-MRA in the follow-up of multiple PAVMs. According to a study by Kawai et al. [17], localized lesions on MRI and CT in a 1-to-1 manner were difficult and required source images of TR-MRA, and multiplanar reconstructed CT images were necessary. However, the incidence of multiple PAVMs is approximately 36% and is particularly high in patients with hereditary hemorrhagic telangiectasia [19,20]. In this study, single-shot whole thoracic TR-MRA was performed using a 3T machine with higher SNRs and large FOV over 1.5T MRI while preserving spatial and temporal resolutions [14]. Furthermore, the MPR showed a high feeding artery matching ratio and good diagnostic accuracy for reperfusion.

There are remaining concerns over feeding arteries that are invisible in TR-MRA. In the present study, the MPR technique was helpful in such cases. However, inter-reader mismatches in pericardiac location and small feeding arteries (< 1.5 mm in diameter) remained even after MPR analysis. These issues have been discussed as limitations of TR-MRA in previous studies [14,17].

Increasing the spatial resolution while maintaining the temporal resolution is the most important factor in reducing non-matching cases caused by a small feeding artery. Hamamoto et al. [21] suggested an ultra-short echo time MRI for PAVM surveillance. Using respiratory gating and ultra-short echo time, they showed high spatial resolution (slice thickness of 1 mm without reconstruction), temporal resolution, and reduced motion artifacts. However, there are some drawbacks, including prolonged acquisition time (7–10 minutes) and lack of hemodynamic information compared to TR-MRA. Ultra-short echo time MR angiography using arterial spin labeling attempted in another study [22] obtained hemodynamic images of treated PAVMs with a high level of temporal resolution (300 ms) and showed strong susceptibility artifacts from the metallic coils. However, it also has the disadvantages of limited spatial resolution compared with CT, small acquisition volume, and long acquisition time (10–12 minutes).

There has been a steady progression of new technologies to improve the spatial and temporal resolution of MR. Compressed sensing is a method to accelerate MRI acquisition by acquiring fewer data through undersampling of k-space [23]. This has the potential to mitigate the time-intensiveness of TR-MRA by shortening the temporal footprint, which is considered a limitation of the view-sharing technique applied in modern TR-MRA [24]. In thoracic imaging, to decrease motion sensitivity and aliasing artifacts, radial sampling of the k-space combined with parallel imaging was introduced in dynamic volumetric MRI [25]. Furthermore, highly constrained projection reconstruction (HYPR) or hybrid HYPR combined with a phase contrast scan or time-of-flight scan has shown improved spatial and temporal resolution [26-28]. Furthermore, recent deep learning reconstruction algorithms have shortened the scan and reconstruction time of MR and have improved the temporal resolution in TR-MRA [29,30]. These technical developments are expected to improve the spatial and temporal resolutions of TR-MRA by reducing imaging artifacts.

Currently, non-enhanced CT is the recommended follow-up modality after PAVM embolization [9,10,13]. However, the widely used 70% vein size reduction criteria have low specificity [12,15]. A recent angiographically confirmed case series showed a gray zone in the indeterminate area of CT vein size reduction criteria [12]. The diagnosis of reperfusion is challenging, particularly for multiple PAVMs. The authors recommend that a diagnostic approach using both CT and TR-MRA is necessary, particularly for multiple PAVMs. If follow-up CT using the 70% criteria demonstrates ambiguous results, TR-MRA can be used as an auxiliary tool for a more accurate diagnosis.

This study has some limitations. First, it was a retrospective study. Second, the interval between CT and TR-MRA varied among study patients. The possibility of the new development of PAVMs in the time between CT and TR-MRA may not be completely excluded. More investigation is warranted to establish an optimal follow-up protocol for PAVM outcomes.

In conclusion, single-shot whole thoracic TR-MRA showed good visibility of the feeding arteries of PAVMs compared with CT, which further improved using MPR technique, and high accuracy for diagnosing reperfusion after embolization. Single-shot whole thoracic TR-MRA may be a feasible method for the follow-up of patients with multiple PAVMs.

https://doi.org/10.3348/kjr.2022.0140

Korean Journal of Radiology
KJR

Availability of Data and Material

The datasets generated or analyzed during the study are available from the corresponding author on reasonable request.

Conflicts of Interest

The authors have no potential conflicts of interest to disclose.

Author Contributions

Conceptualization: Sang Yub Lee. Data curation: Jihoon Hong, Jongmin Park, Jae-Kwang Lim. Formal analysis: Jihoon Hong, Jung Guen Cha. Investigation: Jung Guen Cha, Donghyeon Kim. Methodology: Sang Yub Lee, Jihoon Hong. Project administration: Sang Yub Lee. Resources: Jae-Kwang Lim, Jongmin Park, Jongmin Lee, Hui Joong Lee. Software: Jihoon Hong, Jung Guen Cha. Supervision: Sang Yub Lee, Jongmin Lee. Validation: Sang Yub Lee, Hui Joong Lee. Visualization: Jihoon Hong, Sang Yub Lee. Writing—original draft: Jihoon Hong. Writing—review & editing: Sang Yub Lee.

ORCID iDs

Jihoon Hong
https://orcid.org/0000-0003-3389-244X
Sang Yub Lee
https://orcid.org/0000-0001-8529-8229
Jae-Kwang Lim
https://orcid.org/0000-0002-1299-9996
Jongmin Lee
https://orcid.org/0000-0002-4163-913X
Jongmin Park
https://orcid.org/0000-0001-9240-4181
Jung Guen Cha
https://orcid.org/0000-0002-2519-2120
Hui Joong Lee
https://orcid.org/0000-0002-1279-3795
Donghyeon Kim
https://orcid.org/0000-0002-4600-8062

Funding Statement

None

Acknowledgments

We would like to thank Wade Martin of Emareye Medical Editing for his critical revision of this manuscript.

REFERENCES

1. Tellapuri S, Park HS, Kalva SP. Pulmonary arteriovenous malformations. *Int J Cardiovasc Imaging* 2019;35:1421-1428
2. White RI Jr, Pollak JS, Wirth JA. Pulmonary arteriovenous malformations: diagnosis and transcatheter embolotherapy. *J Vasc Interv Radiol* 1996;7:787-804
3. Shimohira M, Kawai T, Hashizume T, Muto M, Kitase M, Shibamoto Y. Usefulness of hydrogel-coated coils in embolization of pulmonary arteriovenous malformations. *Cardiovasc Intervent Radiol* 2018;41:848-855
4. Lee SY, Lee J, Kim YH, Kang UR, Cha JG, Lee J, et al. Efficacy and safety of AMPLATZER vascular plug type IV for embolization of pulmonary arteriovenous malformations. *J Vasc Interv Radiol* 2019;30:1082-1088
5. Hayashi S, Baba Y, Senokuchi T, Nakajo M. Efficacy of venous sac embolization for pulmonary arteriovenous malformations: comparison with feeding artery embolization. *J Vasc Interv Radiol* 2012;23:1566-1577; quiz 1581
6. Ratnani R, Sutphin PD, Koshti V, Park H, Chamarthy M, Battaile J, et al. Retrospective comparison of pulmonary arteriovenous malformation embolization with the polytetrafluoroethylene-covered nitinol microvascular plug, AMPLATZER plug, and coils in patients with hereditary hemorrhagic telangiectasia. *J Vasc Interv Radiol* 2019;30:1089-1097
7. Tau N, Atar E, Mei-Zahav M, Bachar GN, Dagan T, Birk E, et al. Amplatzer vascular plugs versus coils for embolization of pulmonary arteriovenous malformations in patients with hereditary hemorrhagic telangiectasia. *Cardiovasc Intervent Radiol* 2016;39:1110-1114
8. Woodward CS, Pyeritz RE, Chittams JL, Trerotola SO. Treated pulmonary arteriovenous malformations: patterns of persistence and associated retreatment success. *Radiology* 2013;269:919-926
9. Lee DW, White RI Jr, Egglin TK, Pollak JS, Fayad PB, Wirth JA, et al. Embolotherapy of large pulmonary arteriovenous malformations: long-term results. *Ann Thorac Surg* 1997;64:930-939; discussion 939-940
10. Remy-Jardin M, Dumont P, Brillet PY, Dupuis P, Duhamel A, Remy J. Pulmonary arteriovenous malformations treated with embolotherapy: helical CT evaluation of long-term effectiveness after 2-21-year follow-up. *Radiology* 2006;239:576-585
11. Bélanger C, Chartrand-Lefebvre C, Soulez G, Faughnan ME, Tahir MR, Giroux MF, et al. Pulmonary arteriovenous malformation (PAVM) reperfusion after percutaneous embolization: sensitivity and specificity of non-enhanced CT. *Eur J Radiol* 2016;85:150-157
12. Hong J, Lee SY, Cha JG, Lim JK, Park J, Lee J, et al. Pulmonary arteriovenous malformation (PAVM) embolization: prediction of angiographically-confirmed recanalization according to PAVM diameter changes on CT. *CVIR Endovasc* 2021;4:16
13. Faughnan ME, Palda VA, Garcia-Tsao G, Geisthoff UW,

 https://doi.org/10.3348/kjr.2022.0140

McDonald J, Proctor DD, et al. International guidelines for the diagnosis and management of hereditary haemorrhagic telangiectasia. *J Med Genet* 2011;48:73-87
14. Kawai T, Shimohira M, Kan H, Hashizume T, Ohta K, Kurosaka K, et al. Feasibility of time-resolved MR angiography for detecting recanalization of pulmonary arteriovenous malformations treated with embolization with platinum coils. *J Vasc Interv Radiol* 2014;25:1339-1347
15. Shimohira M, Kawai T, Hashizume T, Ohta K, Nakagawa M, Ozawa Y, et al. Reperfusion rates of pulmonary arteriovenous malformations after coil embolization: evaluation with time-resolved MR angiography or pulmonary angiography. *J Vasc Interv Radiol* 2015;26:856-864.e1
16. Shimohira M, Kiyosue H, Osuga K, Gobara H, Kondo H, Nakazawa T, et al. Location of embolization affects patency after coil embolization for pulmonary arteriovenous malformations: importance of time-resolved magnetic resonance angiography for diagnosis of patency. *Eur Radiol* 2021;31:5409-5420
17. Kawai T, Shimohira M, Ohta K, Hashizume T, Muto M, Suzuki K, et al. The role of time-resolved MRA for post-treatment assessment of pulmonary arteriovenous malformations: a pictorial essay. *Cardiovasc Intervent Radiol* 2016;39:965-972
18. Pierucci P, Murphy J, Henderson KJ, Chyun DA, White RI Jr. New definition and natural history of patients with diffuse pulmonary arteriovenous malformations: twenty-seven-year experience. *Chest* 2008;133:653-661
19. Gossage JR, Kanj G. Pulmonary arteriovenous malformations. A state of the art review. *Am J Respir Crit Care Med* 1998;158:643-661
20. Saboo SS, Chamarthy M, Bhalla S, Park H, Sutphin P, Kay F, et al. Pulmonary arteriovenous malformations: diagnosis. *Cardiovasc Diagn Ther* 2018;8:325-337
21. Hamamoto K, Chiba E, Oyama-Manabe N, Yuzawa H, Shinmoto H. Assessment of pulmonary arteriovenous malformation with ultra-short echo time magnetic resonance imaging. *Eur J Radiol* 2022;147:110144
22. Hamamoto K, Chiba E, Oyama-Manabe N, Shinmoto H. Ultra-short echo time magnetic resonance angiography using a modified signal targeting with alternative radio frequency spin labeling technique for detecting recanalized pulmonary arteriovenous malformation after coil embolization. *Acta Radiol Open* 2021;10:2058460121105767
23. Jaspan ON, Fleysher R, Lipton ML. Compressed sensing MRI: a review of the clinical literature. *Br J Radiol* 2015;88:20150487
24. Rapacchi S, Han F, Natsuaki Y, Kroeker R, Plotnik A, Lehrman E, et al. High spatial and temporal resolution dynamic contrast-enhanced magnetic resonance angiography using compressed sensing with magnitude image subtraction. *Magn Reson Med* 2014;71:1771-1783
25. Feng L, Grimm R, Block KT, Chandarana H, Kim S, Xu J, et al. Golden-angle radial sparse parallel MRI: combination of compressed sensing, parallel imaging, and golden-angle radial sampling for fast and flexible dynamic volumetric MRI. *Magn Reson Med* 2014;72:707-717
26. O'Halloran RL, Wen Z, Holmes JH, Fain SB. Iterative projection reconstruction of time-resolved images using highly-constrained back-projection (HYPR). *Magn Reson Med* 2008;59:132-139
27. Velikina JV, Johnson KM, Wu Y, Samsonov AA, Turski P, Mistretta CA. PC HYPR flow: a technique for rapid imaging of contrast dynamics. *J Magn Reson Imaging* 2010;31:447-456
28. Wu Y, Kecskemeti SR, Johnson K, Wang K, Rowley H, Wieben O, et al. HYPR TOF: time-resolved contrast-enhanced intracranial MR angiography using time-of-flight as the spatial constraint. *J Magn Reson Imaging* 2011;33:719-723
29. Cha E, Chung H, Kim EY, Ye JC. Unpaired training of deep learning tMRA for flexible spatio-temporal resolution. *IEEE Trans Med Imaging* 2021;40:166-179
30. Cha E, Kim EY, Ye JC. K-space deep learning for parallel MRI: application to time-resolved MR angiography. arXiv [Preprint]. 2018 [cited May 27, 2022]. Available at: https://doi.org/10.48550/arXiv.1806.00806

https://doi.org/10.3348/kjr.2022.0140